Conducting Materials

DOI: 10.1002/ange.200600553

A High-Conductivity Crystal Containing a Copper(I) Coordination Polymer Bridged by the Organic Acceptor TANC**

Makoto Tadokoro, Syuma Yasuzuka, Masaharu Nakamura, Takumi Shinoda, Toshinori Tatenuma, Minoru Mitsumi, Yoshiki Ozawa, Koshiro Toriumi, Harukazu Yoshino, Daisuke Shiomi, Kazunobu Sato, Takeji Takui, Takehiko Mori, and Keizo Murata*

Artificial conductors constructed from molecular building blocks can replicate unique low-dimensional electron-transport phenomena depending on the nature of their molecular components.[1] For example, $Cu(DCNQI)_2$ (DCNQI = *N*,*N*′-dicyanoquinodiimine) systems formed from coordination polymers containing alternating 3D linkages between Cu ion donors and organic DCNQI acceptors exhibit an interesting metal–insulator (M–I) transition under high pressure. This behavior is due to the interaction between the localized 3d-electron bands of the Cu ions and the π-electron conductive bands of DCNQI.[2] Therefore, the appropriate combination of donors and acceptors as molecular building blocks, which often form an electron-conducting solid, plays an important role in determining the electron-transport character of a molecular crystal.

Molecules that form high-conductivity molecular solids, particularly organic acceptors, have been limited thus far to cyanoquinoid derivatives such as TCNQ[3] and DCNQI[4] and the metal complex $[M(dmit)_2]$ (dmit = 1,3-dithiole-2-thioxo-4,5-dithiolato).[5] Molecular conductors with various electron-donor frameworks based on heterocyclic structures containing a chalcogen atom such as tetrathiafulvalene (TTF)[6] and tetramethyltetraselenofulvalene (TMTSF)[7] have also been realized, and studies are underway to discover a fundamental molecule with a stable electron-accepting framework to form molecular conductors with a desired transport behavior. Herein, we report a modifiable electron acceptor with 5,6,11,12-tetraazanaphthacene (TANC) as a new fundamental framework and the preparation of a high-conductivity crystal (**1**) from Cu^I–TANC coordination polymers.

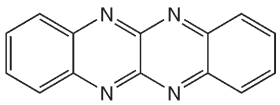

TANC

TANC was prepared by modifying a synthetic procedure first reported by Hill.[8] The yellow precipitate obtained from the thermal condensation between *o*-phenylenediamine and oxamide contains 2,2′-bibenzimidazole and 5,11-dihydro-5,6,11,12-tetraazanaphthacene (FFV) in a 3:1 ratio. This mixture was oxidized with PbO_2 in MeCN to give brown crystals of TANC in 20% yield. The cyclic voltammogram of TANC in MeCN exhibits two reversible one-step, one-electron waves in the reverse sweep ($E^1_{1/2} = -0.20$ and $E^2_{1/2} = -0.88$ V vs Ag/AgCl), which means that TANC is a weaker electron acceptor than organic acceptors such as TCNQ and DCNQI that form high-conductivity materials.[9] Unfortunately, TANC cannot be employed as an organic semiconductor with n-type characteristics.

The TANC radical anion can be isolated from an electron disproportionate reaction between FFV and TANC under basic conditions. This compound was obtained as a green precipitate under anaerobic conditions, which immediately turns gray upon exposure to air. The ESR spectrum of the precipitate exhibits a typical anisotropic peak ($g_\perp = 2.011$ and $g_\parallel = 2.0091$) that stabilizes at room temperature (see the Supporting Information).

The high-conductivity crystal **1**, which has the composition $[\{Cu(TANC)\}F_{0.5}]_n$, was obtained from the reaction between TANC and $[Cu(MeCN)_4]BF_4$ in MeOH/MeCN in the form of thin, plate-like, indigo-blue crystals. The presence of half an equivalent of nonstoichiometric F^- ions was determined by X-ray photoelectron spectroscopy (XPS) measurements and quantitative chemical analysis for F^- ions. These F^- ions are generated by the dissociation of BF_4^- anions in the reaction mixture.

Direct electron-conductivity measurements for a single crystal of **1** were performed by the conventional four-probe dc method by varying the temperature (Figure 1). The crystals

[*] Prof. M. Tadokoro, T. Shinoda, T. Tatenuma
Department of Chemistry
Faculty of Science
Tokyo University of Science
Kagurazaka 1-3, Shinjuku-ku, Tokyo 162-8601 (Japan)
Fax: (+81) 3-5228-8714
E-mail: tadokoro@rs.kagu.tus.ac.jp
Dr. M. Mitsumi, Prof. Y. Ozawa, Prof. K. Toriumi
Department of Chemistry
Faculty of Science
Hyogo Prefecture University
Kouto 3-2-1, Kamikouri-cho, Akou-gun 678-1297 (Japan)
Dr. S. Yasuzuka, M. Nakamura, Dr. H. Yoshino, Prof. D. Shiomi, Prof. K. Sato, Prof. T. Takui, Prof. K. Murata
Department of Chemistry and Department of Material Sciences
Graduate School of Science
Osaka City University
Sugimoto 3-3-138, Sumiyoshi-ku, Osaka 558-8585 (Japan)
Prof. T. Mori
Department of Organic Polymeric Materials
Interdisciplinary Graduate School of Science and Engineering
Tokyo Institute Technology
Nagatsuda-cho 4259, Midori-ku, Yokohama 226-8502 (Japan)

[**] This study was supported by a Grant-in-Aid for Scientific Research on Priority Areas (nos. 16041237 and 16038221) and Scientific Research (B) (no. 16350034) from the Ministry of Education, Culture, Science and Technology of Japan. The authors are grateful for time on the BL02B1 beamline of the SPring-8 facility and thank the Analytical Center of Osaka City University for providing the CCD X-ray diffractometer and performing the elemental analysis.
TANC = 5,6,11,12-tetraazanaphthacene.

Supporting Information for this article is available on the WWW under http://www.angewandte.org or from the author.

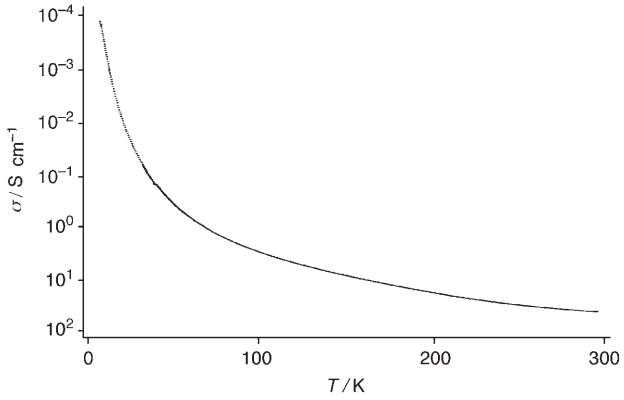

Figure 1. Temperature-dependent conductivity of **1** at ambient pressure using the typical four-probe dc method. The measurement was performed by attaching an Au wire ($\phi = 10\ \mu m$) to the (001) face in a crystal of **1** ($0.78 \times 0.22 \times 0.03\ mm^3$).

exhibit a high conductivity of $50\ S\,cm^{-1}$ along the *a* axis at 300 K, and the conductivity sinks rapidly to $10^{-6}\ S\,cm^{-1}$ at 10 K, with a decrease in temperature. This behavior implies that **1** is a semiconductor at ambient pressure.

An X-ray structure analysis was performed for a platelike single crystal of **1** ($0.41 \times 0.15 \times 0.03\ mm^3$).[10] Figure 2a shows a flat-ribbon structure with alternative linkages between the Cu^+ ions and TANC along the *b* axis. Two of the four N atoms in the TANC framework, namely N(1) and N(1)*[1] ("*1": $-x$, $-y$, $-z$), are coordinated to two different Cu^+ ions. The coordination structure around each Cu^+ ion is approximately linear didentate (Cu(1)–N(1) = 1.887(5) Å). The two remaining non-coordinating atoms (N(2) and N(2)*) reinforce the coordination structure through weak C–H···N hydrogen bonds (N(2)···C(2)*[2] = 3.772(9) Å; "*2": $x-1$, $y+1$, z). They

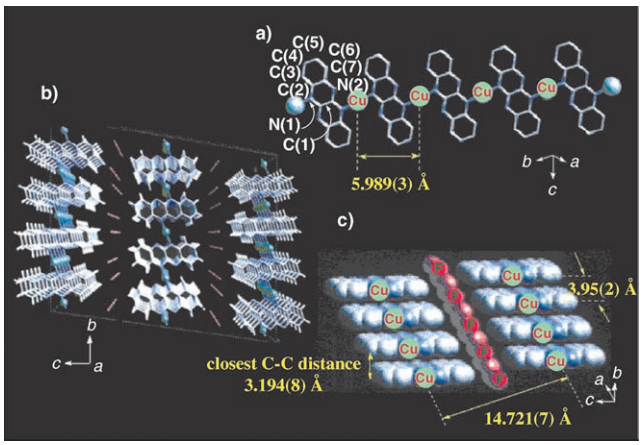

Figure 2. a) The structure of the oblique one-dimensional coordination polymer in **1** with alternating linkages between Cu^+ ions and TANC showing the shortest Cu–Cu distance in the intrapolymer chain (5.989(3) Å); b) the segregated stacking of the coordination polymer along the *a* axis to create two-dimensional stacking layers, which are separated by other layers constructed from disordered F^- ions (pink spheres) along the *c* axis; c) a perspective view along the *a* axis showing the stacking Cu–Cu distances (3.9451(2) Å), the shortest C–C distance (3.19 Å) between the stacking TANC molecules, and the shortest interlayer Cu–Cu stacking distance (14.721(7) Å).

also affect the electron structure of the Cu^+ ion by a weak contact interaction. This interaction originates because the lone-pair electrons of the N(2) and N(2)* atoms are directed toward the Cu^+ ion despite a long noncoordinating distance of 2.853(5) Å between Cu(1) and N(2).

The flat-ribbon structures are arranged in segregated stacks for each fragment of Cu^+ ions and TANC along the *a* axis in **1** to form 2D stacking layers (Figure 2b). The shortest C–C distance between the stacked TANC molecules within the layers is that between C(1) and C(7)*[3] (3.184(9) Å; "*3": $-x$, $-y+1$, $-z$). Few direct Cu–Cu interactions exist between the ribbons in the layer because the shortest Cu(1)–Cu(1)* distance is 3.95(2) Å, which is greater than the total van der Waals radius between two Cu^+ ions. The nonstoichiometric F^- ions are located in the spaces between the layers in a single unit separate the conductive layers along the *c* axis (Figure 2c).

Conductivity anisotropy measurements were performed for **1** at room temperature for the crystal directions (100) and (010) using the Montgomery method.[11] The conductivity, σ_c, is $6.90 \times 10^{-3}\ S\,cm^{-1}$ for the (001) direction, which corresponds to the smallest edge length among the three planes. This value is smaller by four and two orders of magnitude than σ_a ($50.0\ S\,cm^{-1}$ for the (100) direction) and σ_b ($0.91\ S\,cm^{-1}$ for the (010) direction), respectively. This variation occurs due to the alternating layers of F^- ions that disturb the conductivity through the (001) direction, which means that the crystal behaves as an approximate pseudo-1D molecular semiconductor based on the layer stacking along the *ab* plane; the maximum amount of current flows through the 1D stacked TANC arrays along the *a* axis.

This behavior as a 1D molecular conductor can also be explained by extended Hückel calculations based on the crystal structure of **1**.[12] If the Cu atoms are not considered, the LUMO band of the TANC molecules shows the following intermolecular overlaps: 7.1×10^{-3} for the stacking direction of the *a* axis and 0.7×10^{-3} for the interchain direction of the *b* axis. This yields a 1D energy band along the stacking *a* axis with a bandwidth of 0.28 eV and an interchain interaction one-tenth that of the intrachain interaction. The tight-binding approximation of the LUMO band yields a 1D energy band and an open Fermi surface (Figure 3a).

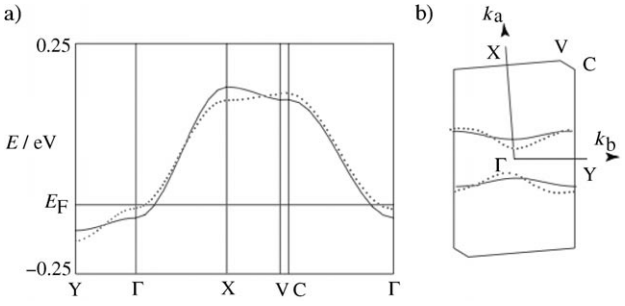

Figure 3. a) The energy dispersion and b) the Fermi surface of a crystal of **1** calculated by the extended Hückel method with a tight-binding approximation. The black line represents the energy band calculated using only the TANC π band and the dotted line represents the energy band obtained by considering the π–d interchain interactions of the hybridization between Cu ions and the TANC LUMO ($t_\perp = 0.01$ eV).

The whole band calculation, including the Cu orbitals, shows that the Cu 3d bands are located around the HOMO band and are completely occupied (Figure 3b). This result is consistent with the existence of only Cu^+ species (absence of Cu^{2+}), as observed by XPS. Furthermore, the nearly temperature-independent spin susceptibility of **1** is regarded as being Pauli-like, which also indicates the absence of Cu^{2+} species. The density of the $S = 1/2$ local spin was estimated to be 1.15% from the Curie tail (see the Supporting Information). Owing to the coordination of the TANC molecules to the Cu atom, the orbital overlap between the TANC LUMO and the Cu orbitals is considerable: 7.5×10^{-3} to the Cu 3d orbitals and 17.3×10^{-3} to the Cu 4p orbitals. However, the hybridization of the Cu 3d orbitals with the TANC LUMO is weak because the 3d levels are located entirely below the LUMO level.

As the Cu 3d orbitals are separated from the LUMO level by more than 1 eV, the Cu 3d–LUMO hybridization yields $t_\perp = 2 \times 0.0752/\Delta = 0.01$ eV for the indirect interchain interaction between the TANC molecules through the Cu atom. These values are similar in order to those for the direct interchain interaction between the TANC molecules and are consistent with the results of the conductivity anisotropy measurements. The tight-binding energy band including this indirect interaction is depicted in Figure 3b, which shows that the 1D band remains essentially unchanged. Therefore, the Cu 3d orbitals do not contribute significantly to the interchain interaction because the Cu atom exists as Cu^+.

Plots of the resistivity against $1/T$ for **1** yield a roughly curved line, which indicates a behavior different from that of a typical thermally excited semiconductor (see the Supporting Information). Therefore, the temperature-dependent resistivity of **1** at high pressure was measured up to approximately 8 GPa by using a cubic anvil apparatus.[13,14] The resistivity increases uniformly until approximately 6.5 GPa, and it decreases slightly at 8 GPa (see the Supporting Information). This variation in the insulating behavior with pressure for **1** is similar to that of Cu–DCNQI systems, which also exhibit an increase in resistivity under high pressure.[15] The sharp decrease in the resistivity above 6.5 GPa at 300 K may be attributed to the enhanced overlap of π orbitals in TANC molecules. However, it is difficult to understand the pressure-enhanced insulating state. The temperature dependence of the resistivity can be well fitted by the variable-range-hopping (VRH) formula even under high pressures,[16] which suggests that the spatially disordered F^- ions play an important role in the electron-transport behavior of **1**. We therefore require a model different from that of the Cu–DCNQI system to understand the pressure-enhanced insulating behavior. The large conductivity anisotropy ($\sigma_a/\sigma_b/\sigma_c \approx 7000{:}117{:}1$) suggests that the energy levels of the Cu 4s and 3d orbitals are significantly higher and lower than that of the TANC LUMO, respectively. Hence, the Cu^+ ions make no contribution to the conduction band. This implies that the hybridization between the Cu 3d orbital and the TANC LUMO is negligible at ambient pressure. The random potential generated by the spatially disordered F^- ions may become stronger upon application of pressure because the distance between the layers with stacked TANC columns and those with disordered F^- ions decreases with an increase in pressure. As a result, the application of pressure may increase the purity of the one-dimensionality and the strength of the random potential as a result of disordered F^- ions. In other words, the 1D VRH is enhanced with an increase in pressure up to 6.5 GPa.

We have reported the preparation of a new high-conductivity crystal **1**, which is constructed from coordination polymers containing Cu^+ ions and novel TANC acceptors. By employing the simple fundamental framework of TANC, it should be possible to convert the crystal structure into that of other analogues and introduce a variety of substituented groups such as a series of TCNQ and DCNQI acceptors. Furthermore, according to the measurements of the temperature-dependent resistivity under high pressure and the conductivity anisotropy, it seems likely that the conduction mechanism of **1** follows the 1D VRH formula based on the disordered F^- ions, which affects the stacking of the TANC columns below 6.5 GPa. It should be possible to establish the mechanism for the decrease in resistivity above 6.5 GPa by preparing other Cu molecular conductors with TANC derivatives.

Experimental Section

1: $[Cu(MeCN)_4]BF_4$ (0.34 g, 1.0 mmol) and TANC (40 mg, 0.17 mmol) were mixed in MeCN (36 mL) and stirred for 10 min. The solution was filtered and divided into 18 × 2-mL portions. MeOH (8 mL) was added to each portion and the mixture was slowly evaporated at room temperature. Deep-blue crystals were deposited from the concentrated solution as thin, platelike rhombuses. Yield: 25.0 mg (50%). Elemental analysis (%) for $C_{14}H_8CuF_{0.5}N_4$: calcd C 55.08, H 2.64, Cu 20.81, F 3.11, N 18.35; found C 55.33, H 2.64, Cu 20.73, F 3.40, N 18.41.

Received: February 10, 2006
Revised: April 24, 2006

Keywords: conducting materials · copper · crystal engineering · high-pressure chemistry · supramolecular chemistry

[1] Special issue on organic conductors: *Chem. Rev.* **2004**, *104*, 4887–5782.
[2] a) R. Kato, *Bull. Chem. Soc. Jpn.* **2000**, *73*, 515; b) M. Tamura, Y. Kashimura, H. Sawa, S. Aonuma, R. Kato, M. Kinoshita, *Solid State Commun.* **1995**, *93*, 585; c) Y. Kashimura, H. Sawa, S. Aonuma, R. Kato, H. Takahashi, N. Mori, *Solid State Commun.* **1995**, *93*, 675.
[3] J. Ferraris, D. O. Cowan, V. Walatka, Jr., J. H. Perlstein, *J. Am. Chem. Soc.* **1973**, *95*, 948.
[4] A. Aumüller, P. Erk, G. Klebe, S. Hünig, J. U. von Schütz, H.-P. Werner, *Angew. Chem.* **1986**, *98*, 759; *Angew. Chem. Int. Ed. Engl.* **1986**, *25*, 740.
[5] L. Brossard, M. Ribault, L. Valade, P. Cassoux, *J. Phys.* **1989**, *50*, 1521.
[6] F. Wudl, R. C. Haddon, E. T. Zellers, F. B. Bramwell, *J. Org. Chem.* **1979**, *44*, 2291.
[7] D. Jerome, A. Mazaud, M. Ribault, K. Bechgaard, *J. Phys. Lett.* **1984**, *39*, 12.
[8] J. H. M. Hill, *J. Org. Chem.* **1963**, *28*, 1931.
[9] A. Aumüller, S. Hünig, *Liebigs Ann. Chem.* **1986**, 142.
[10] Single-crystal data for **1** at 20°C: $C_{14}H_8CuF_{0.5}N_4$, $M_w = 305.29$, triclinic, space group $P\bar{1}$ (no. 2), $a = 3.9521(2)$, $b = 5.989(3)$, $c = 14.721(7)$ Å, $\alpha = 81.29(2)$, $\beta = 85.71(2)$, $\gamma = 84.87(2)°$, $V =$

342.3(3) Å^3, $Z=1$, $\rho_{calcd}=1.481$ g cm^{-3}, $\mu(Mo_{K\alpha})=15.93$ cm^{-1}. A total of 1459 ($R_{int}=0.039$) independent reflections having $2\theta<54.9°$ were collected. The resulting parameters were refined to converge at R_1 (based on F_o) $=0.074$ for 105 parameters ($I>4.00\sigma(I)$ for $2\theta<54.9°$) on 1193 reflections. Max./min. residual electron density 1.98/−0.58 e Å^{-3}; GOF = 1.64. The data collection for **1** was performed with a computer-controlled Rigaku/MSC Mercury CCD auto-diffractometer using Lorenz-polarization corrections and graphite-monochromated $Mo_{K\alpha}$ radiation ($\lambda=0.71069$ Å). The structures were solved by direct methods with SIR92[17] and full-matrix least-squares (DIRDIF99) refinement.[18] The hydrogen-atom positions were fixed. Further details of the data collection and structure solution of **1** are provided as Supporting Information. CCDC-297950 contains the supplementary crystallographic data for this paper. These data can be obtained free of charge from the Cambridge Crystallographic Data Center via www.ccdc.cam.ac.uk/data request/cif.

[11] H. C. Montgomery, *J. Appl. Phys.* **1971**, *42*, 2971.

[12] T. Mori, A. Kobayashi, Y. Sasaki, H. Kobayashi, G. Saito, H. Inoguchi, *Bull. Chem. Soc. Jpn.* **1984**, *57*, 627.

[13] H. Taniguchi, M. Miyashita, K. Uchiyama, K. Satoh, N. Mori, H. Okamoto, K. Miyagawa, K. Kanoda, M. Hedo, Y. Uwatoko, *J. Phys. Soc. Jpn.* **2003**, *72*, 468.

[14] a) S. Yasuzuka, K. Murata, H. Yoshino, T. Fujimoto, M. Shimotori, M. Nakamura, M. Tadokoro, *J. Phys. Soc. Jpn.* **2005**, *75*, 14704; b) S. Yasuzuka, K. Murata, T. Fujioto, M. Shimotori, K. Yamaya, *J. Phys. Soc. Jpn.* **2005**, *74*, 1782.

[15] a) T. Mori, H. Inokuchi, A. Kobayashi, R. Kato, H. Kobayashi, *Phys. Rev. B* **1988**, *38*, 5913; b) T. Takahashi, K. Kanoda, T. Tamura, K. Hiraki, K. Ikeda, R. Kato, H. Kobayashi, A. Kobayashi, *Synth. Met.* **1993**, *56*, 2281; c) A. Kawamoto, K. Miyagawa, K. Kanoda, *Phys. Rev. B* **1998**, *58*, 1243.

[16] a) N. F. Mott, *Proc. Phys. Soc. London Sect. A* **1949**, *62*, 416; b) N. F. Mott, *Metal–Insulator Transitions*, *2nd ed.*, Taylor and Francis, London, **1990**.

[17] A. Altomare, G. Cascarano, C. Giacovazzo, A. Guagliardi, M. Burla, G. Polidori, M. Camalli, *J. Appl. Crystallogr.* **1994**, *27*, 435.

[18] P. T. Beuskens, G. Admiraal, G. Beurskens, W. P. Bosman, R. de Gelder, R. Israel, J. M. M. Smits, The DIRDIF-99 program system, Technical Report of the Crystallography Laboratory, University of Nijmegen, The Netherlands, **1999**.

